BEHAVIOR OF A THREE-LAYER CYLINDRICAL SHELL CONNECTED TO RIGID MASSES UNDER THE INFLUENCE OF ACOUSTIC PRESSURE WAVES

É. I. Grigolyuk and E. B. Kuznetsov

UDC 533.6.013.42

We proposed to investigate a three-layer cylindrical shell connected at the ends to two hemispherical bodies having masses m_1 and m_2 and not exceeding the outside dimensions of the shell. The shell is reinforced with two rigid ribs of mass m_3 and m_4, to which is connected via elastic elements a body of mass m executing reciprocating motion. A plane acoustic pressure wave, its front perpendicular to the axis of the system so described, impinges on the structure, which is immersed in an ideal compressible fluid. The first element encountered by the wave is the hemispherical mass m_1, followed by the cylindrical shell with the reinforcing member m_3. The behavior of the structure is analyzed in time intervals such that the hydrodynamic influence of the bodies m_1 and m_2 on one another can be neglected. The hydrodynamic pressure acting on the structure is determined approximately without regard for diffraction effects from the ribs. The structure is investigated in the neutral buoyancy state.

The analogous problem for the motion of a body of revolution coupled with a semi-infinite elastic rod under the influence of a plane acoustic wave is discussed in [1]. The authors [2] have analyzed the behavior of a homogeneous cylindrical shell end-coupled with rigid bodies of revolution, on which are spring-mounted point masses. Moshenskii [3] discusses the behavior of a cylindrical shell with rigid diaphragms at the ends and with masses attached to it at a certain point via elastic elements; a rod model is used to describe the motion of the shell, i.e., the radial displacements are ignored, and it is assumed that the motion of the oscillators does not affect the motion of the shell.

1. The analysis of the behavior of the given shell is based on the nonlinear equilibrium equations for three-layer nonsloping shells having an asymmetrical configuration [4]. The equations of motion are derived with regard for the inertial forces in the radial and tangential directions, as well as the rotational inertia of the filler. Let u, w, and Ψ be, respectively, the axial displacement, bending deflection, and shear angle in the filler; then the equations of motion of the cylindrical shell in terms of the forces have the form

$$\frac{\partial N_1}{\partial \xi} + \frac{(1-\nu^2)}{k}\frac{\partial p^* W}{\partial \xi} = \gamma_1 \frac{\partial^2 U}{\partial \tau^2};$$
$$\frac{k}{6}\frac{\partial^2 M}{\partial \xi^2} - N_2 + \frac{\partial}{\partial \xi}\left(N_1 \frac{\partial W}{\partial \xi}\right) - \frac{p^*(1-\nu^2)}{k^2}\left(1 + \frac{\partial U}{\partial \xi} + W\right) = \gamma_1 \frac{\partial^2 W}{\partial \tau^2};$$
$$\frac{k}{6}\frac{\partial H}{\partial \xi} - k_2 Q = \gamma_2 \frac{\partial^2 \Psi}{\partial \tau^2}, \tag{1.1}$$

where

$$U = u/h;\ W = w/h;\ k = h/R;\ k_1 = h_3/2R;\ \tau = ct/R;\ p^* = p/E;\ k_2 = (1-\nu^2)\times$$
$$\times Gt_3/Ek;\quad \gamma_1 = c^2(1-\nu^2)\sum_{i=1}^{3}\rho_i t_i/E;\quad \gamma_2 = c^2(1-\nu^2)k_1^2(\rho_1 t_1 + \rho_2 t_2 + 1/3\rho_3 t_3)/Ek;$$
$$t_i = h_i/h;\qquad i = 1, 2, 3,$$

$h = \sum_{i=1}^{3} h_i$ is the thickness of the three-layer shell, h_i denotes the thicknesses of the layers (i = 1 for the outer supporting layer, i = 2 for the inner layer, and i = 3 for the filler), c is the speed of sound in the medium, t

Moscow. Translated from Zhurnal Prikladnoi Mekhaniki i Tekhnicheskoi Fiziki, No. 2, pp. 183-188, March-April, 1975. Original article submitted March 6, 1974.

is the time, R is the radius of the undisturbed surface of the shell, p is the excess pressure at the incident wave front, E and ν are the reduced elastic modulus and Poisson ratio of the three-layer shell (for which expressions are given in [4]), G is the shear modulus of the filler material, ρ_i denotes the densities of the shell layers, ξ is the longitudinal coordinate referred to the shell radius R, N_1 and N_2 are the dimensionless specific axial and circumferential forces, Q is the transverse force in the filler, and M and H are the dimensionless specific torques, which are expressed in terms of the displacements as follows:

$$
\begin{aligned}
&N_1 = e + \nu W + (c_{12}\alpha + c_{13}\varkappa)/2;\\
&N_2 = W + \nu e + \nu(c_{12}\alpha + c_{13}\varkappa)/2;\\
&M = 3c_{13}(e + \nu W) + (c_{32}\alpha_1 + c_{33}\varkappa)/2;\\
&H = 3c_{12}(e + \nu W) + (c_{22}\alpha_1 + c_{23}\varkappa)/2;\\
&Q = \Psi + k\frac{\partial W}{\partial \xi},
\end{aligned}
\tag{1.2}
$$

where

$$
\begin{aligned}
&e = \frac{\partial U}{\partial \xi} + k\left[\left(\frac{\partial U}{\partial \xi}\right)^2 + \left(\frac{\partial W}{\partial \xi}\right)^2\right]\Big/2;\\
&\alpha = \frac{\partial \Psi}{\partial \xi} + k\frac{\partial^2 W}{\partial \xi^2};\quad \varkappa = -k\frac{\partial^2 W}{\partial \xi^2};\\
&\alpha_1 = \left(\frac{\partial \Psi}{\partial \xi} + k\frac{\partial^2 W}{\partial \xi^2}\right)\left(1 + k\frac{\partial U}{\partial \xi}\right).
\end{aligned}
\tag{1.3}
$$

All ensuing calculations are carried out on the basis of the system of equations (1.1) with allowance for the displacement expressions (1.2) and (1.3). Because of its bulkiness we shall not write out the complete system.

The equations of motion of the rigid bodies have the form

$$
\begin{aligned}
&\ddot{X}_1 = a_1 N_1 + \sum_{i=1}^{3} Q_{1i}^*;\\
&\ddot{X}_2 = -a_2 N_2 - Q_{23}^*;\\
&\ddot{X}_3 = -a_3(N_{3-} - N_{3+}) - \varkappa_3(X_3 - X) - \varepsilon_3(\dot{X}_3 - \dot{X});\\
&\ddot{X}_4 = -a_4(N_{4-} - N_{4+}) - \varkappa_4(X_4 - X) - \varepsilon_4(\dot{X}_4 - \dot{X});\\
&\ddot{X} = \omega_3(X_3 - X) + \omega_4(X_4 - X) + \varepsilon_1(\dot{X}_3 - \dot{X}) + \varepsilon_2(\dot{X}_4 - \dot{X}).
\end{aligned}
\tag{1.4}
$$

The differentiation is with respect to the dimensionless time τ; X_j and X are the displacements of the rigid bodies with masses m_j and m referred to the thickness of the shell h, j = 1, 2, 3, 4; N_j are the dimensionless total longitudinal forces at the contact sites between the shell and the bodies m_j; the minus sign indicates that the force is calculated ahead of the rib, and the plus sign that it is calculated after it;

$$
\begin{aligned}
&Q_{1i}^* = \frac{Q_{1i}R}{m_1 c^2 k};\quad Q_{23}^* = \frac{Q_{23}R}{m_2 c^2 k};\quad a_j = \frac{2\pi R^2 E h}{c^2 m_j(1-\nu^2)};\quad \varkappa_n = \frac{c_n R^2}{m_n c^2};\\
&\omega_n = \frac{c_n R^2}{mc^2};\quad \varepsilon_n = \frac{\nu_n R}{m_n c};\quad \varepsilon_1 = \frac{\nu_3 R}{mc};\quad \varepsilon_2 = \frac{\nu_4 R}{mc};\ j=1,\ 2,\ 3,\ 4;\ n=3,\ 4,
\end{aligned}
$$

where Q_{1i} and Q_{23} are the components of the hydrodynamic forces of the first and second category [5] for the respective bodies m_1 and m_2, c_3 and c_4 are the stiffness coefficients of the springs attaching the body m to the respective ribs m_3 and m_4, and ν_3 and ν_4 are the damping factors. The system of differential equations (1.1) written in terms of the displacements is a system of eighth-order partial differential equations. If we assume that the shell is rigidly clamped at the contact sites with the bodies m_j, we obtain for the boundary conditions

$$
\text{for}\ \xi=\xi_j\ \ \Psi=W=\partial W/\partial\xi=0;\ \ U=X_j,
\tag{1.5}
$$

where ξ_j are the coordinates of the bodies m_j.

The complete system of differential equations of motion (1.4) of the structure, also written in terms of the displacements (1.1), is solved for the null initial conditions

$$
\tau=0,\ \ U=W=\Psi=X=X_j=\dot{U}=\dot{W}=\dot{\Psi}=\dot{X}=\dot{X}_j=0.
\tag{1.6}
$$

Time is reckoned from the instant of encounter of the shock wave with the body m_1.

2. In determining the hydrodynamic forces acting on the structure we use the approximation methods developed in the book [5] and applied in [1-3]. We know that the transient functions $F(\tau)$ characterizing the

pressure variation due to diffraction have significantly nonzero values only in the initial time period equal to the transit time of the pressure wave between the two most distant points of the surface of the body. In this interval the character of the variation of $F(\tau)$ is almost linear. The main idea of the approximative approach is that the transient function $F(\tau)$ is approximated by a linear function

$$F_*(\tau)=(1-\tau/\tau_*)[H(\tau)-H(\tau-\tau_*)], \tag{2.1}$$

in which $H(\ldots)$ is the Heaviside step function and τ_* is a characteristic time determined from the equality of the integrals

$$\int_0^\infty F_*(\tau)\,d\tau=\int_0^\infty F(\tau)\,d\tau,$$

where the last integral is readily computed if the additional mass of the body is known [5]. The problem can thus be solved approximately.

The hydrodynamic loads acting on the body m_1 when the pressure wave $p_1(\xi, \tau)$ impinges on it has the form

$$Q_{11}=-\iint_{s_1} p_1 \cos \mathbf{n}\xi\, ds_1,$$

where s_1 is the part of the surface of the body spanned by the wave and $\mathbf{n}$ is the unit outward normal to the surface of the body;

$$Q_{12}=Q(\tau)-\begin{cases} \dfrac{1}{\tau_*}\displaystyle\int_0^\tau Q(\tau_1)\,d\tau_1, & \tau<\tau_* \\ \dfrac{1}{\tau_*}\displaystyle\int_{\tau-\tau_*}^\tau Q(\tau_1)\,d\tau_1, & \tau\geqslant\tau_*, \end{cases}$$

where $Q(\tau)=\iint_{s_1} p_1 \cos \mathbf{n}\xi\, ds_1$ is the load generated on the surface of the body under the action of the reflected pressure wave in accordance with the hypothesis of plane reflection;

$$Q_{13}=-Q_0\int_0^\tau \ddot{X}_1(\tau-\tau_1)F(\tau_1)\,d\tau_1, \text{ or using (2.1)},$$

$$Q_{13}=\begin{cases} -Q_0\dot{X}_1+Q_0X_1/\tau_* & \tau<\tau_* \\ -Q_0\dot{X}_1+Q_0[X_1-X_1(\tau-\tau_*)]/\tau_* & \tau\geqslant\tau_*, \end{cases}$$

where

$$Q_0=\rho c^2 k\iint_s \cos^2 \mathbf{n}\xi\, ds.$$

Because the analysis is limited to times during which the body m_2 is acted upon only by the radiation pressure associated with its motion, the components Q_{21} and Q_{22} are equal to zero, and Q_{23} is determined the same as Q_{13}. The radiation pressure associated with the motion of the cylindrical shell is calculated on the basis of the thin-layer hypothesis [6]:

$$p=\rho c^2 k\int_0^\tau \ddot{W}(\xi, \tau_1)\exp[-0{,}5(\tau-\tau_1)]\cos 0{,}5(\tau-\tau_1)\,d\tau_1.$$

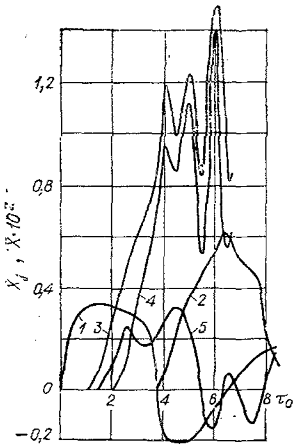

Fig. 1

If a wave with an exponential pressure variation behind the front impinges on the body m_1, i.e.,

$$p_1=p_0\exp(-\delta\tau)H(\tau),$$

where p_0 is the pressure at the wave front and δ is a factor characterizing the rate of change of the pressure behind the front, then the expressions for the hydrodynamic forces of the first category have the form

$$Q_{11}+Q_{12}=2\pi R^2 p_0/\delta\begin{cases} 2(2-\tau)/\delta^2-1/3+2/\delta^3+(1-\tau)[2-\tau+(1-\tau)^2/3] \\ +(2-\tau)^2/\delta-2(1+2/\delta+2/\delta^2+1/\delta^3)\exp(-\delta\tau), & \tau<1; \\ 2\exp(-\delta\tau)[\exp(\delta)(1/\delta+2/\delta^2+2/\delta^3)-1-2/\delta \\ -2/\delta^2-1/\delta^3]-2/\delta^3-(2-\tau)^3/2-(2-\tau)^2/2-2(2-\tau)/\delta^2, & 1\leqslant\tau<2; \\ 2[\exp(\delta)(1/\delta+2/\delta^2+2/\delta^3)-\exp(2\delta)/\delta^3 \\ -2/\delta-2/\delta^2-1/\delta^3-1]\exp(-\delta\tau), & \tau\geqslant 2. \end{cases} \tag{2.2}$$

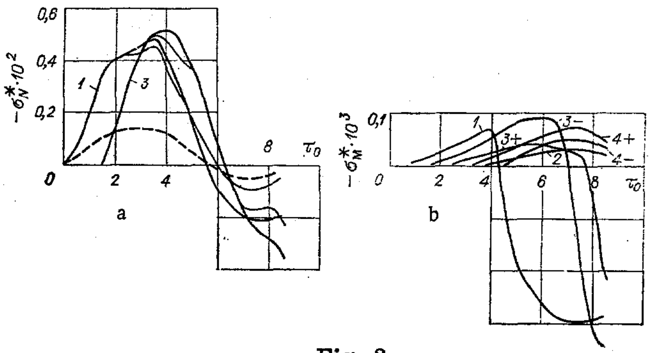

Fig. 2

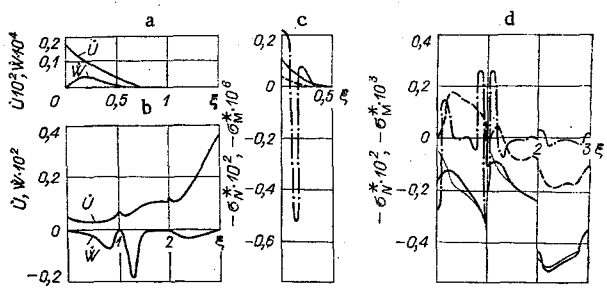

Fig. 3

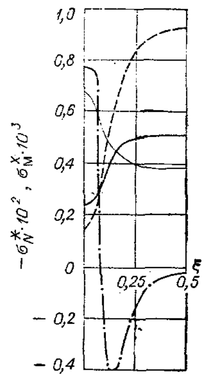

Fig. 4

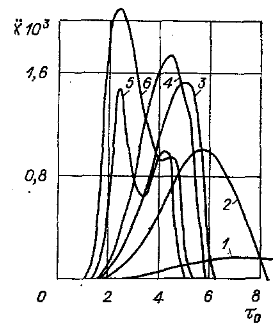

Fig. 5

For the calculation of the hydrodynamic loads we assume that the additional mass of the hemisphere is equal to half the additional mass of the corresponding sphere. If we pass to the limit in (2.2) as δ goes to zero, we obtain expressions for the hydrodynamic loads acting on the hemisphere when a plane step wave is incident upon it [1].

3. The systems of differential equations (1.1) and (1.4) subject to the boundary conditions (1.5) and initial conditions (1.6) are integrated numerically by the Kutta–Merson method after preliminary application of the method of straight lines to the system of equations (1.1). The central differences, which have second-order error, are used. At contour and precontour points the differential operators are also approximated by difference operators with second-order error, with allowance for the boundary conditions. Here the functions U, W, Ψ, $\partial W/\partial \xi$ are represented in the vicinity of the investigated point by Taylor series with as many terms retained as necessary. The expressions given below for the right derivatives at the extreme points are used in formulating the algorithm.

At precontour points:

$$\frac{\partial^3 U}{\partial \xi^3} = \frac{-3U_0 + 10U_1 - 12U_2 + 6U_3 - U_4}{2l^3} + 0\,(l^2);$$

$$\frac{\partial^3 \Psi}{\partial \xi^3} = \frac{10\Psi_1 - 12\Psi_2 + 6\Psi_3 - \Psi_4}{2l^3} + 0\,(l^2);$$

$$\frac{\partial^3 W}{\partial \xi^3} = \frac{-9W_1 + W_3}{3l^3} + 0\,(l^2);$$

$$\frac{\partial^4 W}{\partial \xi^4} = \frac{192W_1 - 108W_2 + 32W_3 - 3W_4}{12l^4} + 0\,(l^2),$$

at contour points:

$$\frac{\partial U}{\partial \xi} = \frac{-3U_0 + 4U_1 - U_2}{2l} + 0\,(l^2);$$

$$\frac{\partial \Psi}{\partial \xi} = \frac{4\Psi_1 - \Psi_2}{2l} + 0\,(l^2); \quad \frac{\partial^2 W}{\partial \xi^2} = \frac{8W_1 - W_2}{2l^2} + 0\,(l^2),$$

where $l = (\xi_2 - \xi_1)/n \cdot n$ and n is the number of partitions of the shell. The subscript j, j = 0, 1, 2, 3, 4, attached to the function indicates that it is calculated at the j-th partition point, j = 0 corresponding to the line of contact of the shell with the body.

The numerical calculations are carried out for a neutral-buoyancy structure immersed in water. The investigated three-layer shell has steel supporting layers ($E_1 = E_2 = 2.3 \cdot 10^6$ kg/cm^2; $\nu_1 = \nu_2 = 0.3$), a lightweight filler transmitting transverse shear ($G = 2400$ kg/cm^2; $E_3 = 0$; $\nu_3 = 0.3$); structural symmetry ($t_1 = t_2 = 0.05$; $t_3 = 0.09$); $k = 0.0464$; $\xi_1 = 0$; $\xi_2 = 3$; $\xi_3 = 1$; $\xi_4 = 2$;: $a_1 = a_2 = 0.865$; $a_3 = a_4 = 8.65$; $\omega_3 = \omega_4 = 5$; $\varepsilon_1 = \varepsilon_2 = \varepsilon_3 = \varepsilon_4 = 0$; $n = 62$; $p_0^* = p_0/E = 0.434 \cdot 10^{-4}$, i.e., it is assumed that the pressure at the front of the incident wave is 10 kg/cm^2.

Figure 1 shows the variations with time $\tau_0 = \tau c_0/c$ of the accelerations of the rigid bodies when the structure is acted upon by a step wave ($\delta = 0$), where c_0 is the speed of sound in the material of the shell. For the case in question $c_0 = 5400$ m/sec; j corresponds to the acceleration of the body m_j, j = 1, 2, 3, 4, and the number 5 corresponds to the acceleration of the body m. It is evident from the figure that at the initial instant the maximum acceleration of the body m is less than the maximum acceleration of m_1 by about 1/1.32. The maximum acceleration of m_2, on the other hand, is about twice the maximum acceleration of the bodies m_1 and m, due to reflection of the stress waves from the right end ($\xi = \xi_2$) of the cylindrical shell. The absolute maximum accelerations are experienced by the ribs due to their relatively small mass. Since damping is ignored ($\varepsilon_j = 0$), the processes have the character of undamped oscillations. An abrupt change in the behavior of the $\ddot{X}_1$ curve takes place at the instant of arrival of the shock wave at the cross section $\xi = \xi_1$. The time variations of the stresses produced at the contact sites between the shell and the rigid masses m_j for the case of an exponential incident pressure wave ($\delta = 3$) are given in Fig. 2. The plus sign after j signifies that the stresses are calculated to the right of the body m_j, and the minus sign that they are calculated to the left of it. The stresses are given in dimensionless form $\sigma_i^* = \sigma_i(1 - \nu^2)/E_i k$, where i = 1 corresponds to the outer supporting layer (heavy curve) and i = 2 to the inner layer (thin curve). Where only one curve is shown it is implied that the stresses in the layers coincide. Figure 2a gives the variation with time τ_0 of the axial (solid curves) and circumferential (dashed curves) membrane stresses, the latter being calculated in the cross section $\xi = \xi_1$. As the figure indicates, the stresses in the layers begin to differ significantly from one another after arrival of the shock wave in the investigated cross section. The circumferential stresses in the layers are practically identical and several times smaller than the axial stresses. The flexural stresses calculated in the outermost fibers, i.e., those furthest from the neutral line of the layers, are given in Fig. 2b. We see that the flexural stresses in the supporting layers practically coincide. The curves experience an abrupt change at the instant of arrival of the shock wave in the investigated cross section. A comparison of Figs. 2a and 2b shows that the membrane stresses in the supporting layers are an order of magnitude greater than the flexural stresses. Plots of the velocities and stresses arising in the shell when the structure is acted upon by a wave with an exponential pressure variation behind the front ($\delta = 3$) are given in Fig. 3 for two times: $\tau_0 = 1$ (a, c) and $\tau_0 = 8.5$ (b, d). The dot-dashed curve corresponds to the flexural stresses, and the rest of the nomenclature is the same as before. It is evident from Figs. 3a and 3b that the velocities $\dot{W}$ of the shell attain their maximum value in the vicinity of the pressure wave front. Figure 3d indicates that at the time $\tau_0 = 8.5$ the axial membrane stresses are tensile in any cross section of the shell, while the cricumferential stresses are compressive in the shell cross sections acted upon by the pressure in the shock wave, and are tensile in the cross sections unperturbed by the pressure wave. The flexural stresses are a maximum in the vicinity of the rib m_3 and the shock-wave front.

It was assumed in the solution presented above that the structure is subjected to equal external and internal pressure and that a shock wave impinges on it. We now consider the case in which the structure has an internal pressure of 1 kg/cm^2 and is submerged in water to a depth of, say, 50 m, i.e., we take into account the external water pressure, which in this case is approximately 5 kg/cm^2. To avoid any appreciable modification of the algorithm we solve the following problem by the relaxation method: A uniform external pressure with an amplitude of 5 kg/cm^2 is applied instantaneously to the structure. As before, the behavior of the system is described by Eqs. (1.1) and (1.4), but now each equation includes a damping term proportional to the velocity. The calculations are carried out in practice until the values of the velocities and accelerations differ from zero in the eighth significant figure. By the symmetry of the problem it is sufficient to consider the half of the shell between the rigid masses, for example the part of the shell between the cross sections $\xi=0$ and $\xi=0.5$. Plots of the stresses for the structure subjected to an external water pressure of 5 kg/cm^2 are given in Fig. 4, which uses the same nomenclature as before. It is evident from the curves for the axial membrane stresses that the stresses in the supporting layers differ considerably from one another. Now to find the stresses in the structure immersed in water when a shock wave impinges on it we must add the result obtained earlier and presented in Figs. 2 and 3 to the results given in Fig. 4.

Finally, we investigate the influence of the stiffness of the coupling of the load m on the behavior of the structure. The time variation of the acceleration of the load when an exponentially decaying pressure wave impinges on the structure is given in Fig. 5 for various values of $\omega_3=\omega_4=\omega$: 1) $\omega=0.01$; 2) $\omega=0.1$; 3) $\omega=0.25$; 4) $\omega=0.5$; 5) $\omega=5$; 6) $\omega_3=\infty$, $\omega_4=0$ (mass m rigidly attached to the rib m_3). The dependence of the maximum acceleration on the coupling stiffness has two maxima for $\omega_3=\infty$ and $\omega=0.5$. The first maximum is caused by the elastic properties of the shell, and the second by the presence of the elastic coupling between the mass m and ribs m_3, m_4. For the assumed parameters of the structure the influence of the coupling stiffness of the load m on the reaction of the masses m_1 and m_2 and on the forces and stresses in the shell is insignificant.

LITERATURE CITED

1. O. A. Frolov, "Longitudinal action of an acoustic pressure wave on a cylindrical rod with a mass of arbitrary configuration at the end," Transactions of the Scientific-Technological Society of the Shipbuilding Industry [in Russian], No. 110, Sudostroenie, Leningrad (1968), p. 31.
2. A. G. Gorshkov and É. I. Grigolyuk, "Action of a plane pressure wave on elastic structures with rigid elements," in: Dynamics of Elastic and Rigid Bodies Interacting with a Fluid [in Russian], Tomsk (1972), pp. 62-72.
3. N. A. Moshenskii, "Longitudinal action of an acoustic pressure wave on a cylindrical shell supporting two elastically coupled masses," in: Problems in the Structural Mechanics of Ships [in Russian], Sudostroenie, Leningrad (1973), pp. 134-142.
4. É. I. Grigolyuk and P. P. Chulkov, Stability and Vibrations of Three-Layer Shells [in Russian], Mashinostroenie, Moscow (1973).
5. B. V. Zamyshlyaev and Yu. S. Yakovlev, Dynamic Loading in Underwater Explosions [in Russian], Sudostroenie, Leningrad (1967).
6. É. I. Grigolyuk and A. G. Gorshkov, "Interaction of weak shock waves with elastic structures," Scientific Transactions of the Institute of Mechanics, Moscow State University [in Russian], No. 13, Moscow (1971).